Blackwell Publishing

Full-length article

Wnt3a signaling promotes proliferation, myogenic differentiation, and migration of rat bone marrow mesenchymal stem cells[1]

Yan-chang SHANG[2,3], Shu-hui WANG[4], Fu XIONG[5], Cui-ping ZHAO[2], Fu-ning PENG[2], Shan-wei FENG[2], Mei-shan LI[2], Yong LI[5], Cheng ZHANG[2,5,6]

[2]Department of Neurology, First Affiliated Hospital, Sun Yat-sen University, Guangzhou 510080,China; [3]Department of Geriatric Neurology, Chinese People's Liberation Army General Hospital, Beijing 100853, China; [4]Department of Neurology, Beijing Friendship Hospital, Capital Medical University, Beijing 100050, China; [5]Center for Stem Cell Biology and Tissue Engineering, Sun Yat-sen University, Guangzhou 510080, China

Abstract

Aim: To investigate the effects of the wingless-related MMTV integration site 3A (Wnt3a) signaling on the proliferation, migration, and the myogenic and adipogenic differentiation of rat bone marrow mesenchymal stem cells (rMSC). **Methods:** Primary MSC were isolated and cultured from Sprague-Dawley rats and characterized by flow cytometry. Mouse L cells were transfected with Wnt3a cDNA, and conditioned media containing active Wnt3a proteins were prepared. Cell proliferation was evaluated by cell count and 5-bromodeoxyuridine incorporation assay. The migration of rMSC was performed by using a transwell migration and wound healing assay. The myogenic and adipogenic differentiation in rMSC were examined by light microscopy, immunofluorescence, and RT–PCR at different time points after myogenic or adipogenic introduction. **Results:** Wnt3a signaling induced β-catenin nuclear translocation and activated the Wnt pathway in rMSC. In the presence of Wnt3a, rMSC proliferated more rapidly than the control cells, keeping their differentiation potential. Moreover, Wnt3a signaling induced 2.62% and 3.76% of rMSC-expressed desmin and myosin heavy chain after being cultured in myogenic medium. The myogenic differentiation genes, including Pax7, MyoD, Myf5, Myf4, and myogenin, were activated after Wnt3a treatment. On the other hand, Wnt3a inhibited the adipogenic differentiation in rMSC through the downregulated expression of CCAAT/enhancer-binding protein alpha (C/EBPalpha) and peroxisome proliferator-activated receptor gamma (PPARgamma). Furthermore, Wnt3a promoted the migration capacity of rMSC. **Conclusion:** The results indicate that Wnt3a signaling can induce myogenic differentiation in rMSC. Wnt3a signaling is also involved in the regulation of the proliferation and migration of rMSC. These results could provide a rational foundation for cell-based tissue repair in humans.

Introduction

Mesenchymal stem cells (MSC), separated from other cells in bone marrow by virtue of their adherence to the plastic walls of tissue culture containers, are capable of differentiating into skeletal muscle cells as well as osteoblasts, chondrocytes, and adipocytes under appropriate culture conditions[1–3]. MSC are also easily obtained from various sources and propagated manifold *ex vivo* to clinically relevant numbers[4]. Furthermore, MSC avoid ethical and immunological hurdles associated with embryonic stem cells, making them attractive candidates for tissue repair and gene therapy[5].

Several studies have shown that transplanted MSC can contribute to muscle cells and restore the sarcolemmal expression of dystrophin in the mdx mouse, a model of Duchenne muscular dystrophy (DMD)[6,7]. MSC as the source of cell therapy to treat muscle diseases are promising

in principle, but the process is rather inefficient when comparing the number of cells implanted with the amount of formed muscle cells. A key to improving the current protocols lies in exploiting the molecular mechanisms governing the distinct steps of myogenic differentiation in MSC[8].

The wingless-related MMTV integration site (Wnt) family includes over 20 cysteine-rich secreted glycoproteins and plays an important role in embryogenesis, including the generation of cell polarity, specification of cell fate, and the regulation of proliferation and differentiation[9,10]. Wnt target gene expression by several different signaling pathways[11]. The canonical pathway is the best characterized at the present time. In the absence of Wnt signaling, β-catenin is phosphorylated by glycogen synthase kinase-3β, in association with axin and adenomatous polyposis coli. These proteins target β-catenin for degradation by the ubiquitin proteasome pathway[12]. When Wnt bind to Frizzled-Low-density lipoprotein receptor-related protein 5/6 (LRP5/6) complex, disheveled protein (a component of the Wnt signaling pathway) is activated and inhibits the phosphorylation of β-catenin. It results in β-catenin stabilization and accumulation in the cytoplasm. The stabilized β-catenin enters the nucleus to bind with members of the T-cell factor (TCF) and lymphoid enhancer factor transcription factor family and induces the expression of target genes[13].

Wnt signaling has been associated with myogenesis in embryogenesis and postnatal muscle regeneration. During embryonic development, Wnt1 and Wnt3a expressed in the dorsal neural tube, and Wnt7a expressed in surface ectoderm, have been shown to activate the expression of myogenic regulatory factor genes in the paraxial mesoderm[14,15]. On the other hand, myogenesis is severely reduced in presomitic mesoderm and newly-formed somites by soluble Frizzled-related proteins that are Wnt antagonists[16]. Furthermore, defects in myogenesis are observed in Wnt1/Wnt3a double-knockout mouse embryos[17]. In postnatal muscle regeneration, it has been shown that Wnt proteins induce myogenic differentiation in CD45+ stem cells[18]. Although these data demonstrate the important roles of Wnt in the regulation of myogenic differentiation in embryogenesis and muscle regeneration, little is known about Wnt signaling inducing myogenic differentiation in bone morrow-derived MSC.

Recent experiments have shown that Wnt signaling has the capacity to promote proliferation and regulate the invasion of human MSC[19]. Moreover, Wnt signaling has an inhibitory effect on osteogenic and adipogenic differentiation in human MSC[20,21]. These studies suggest that Wnt signaling plays a potentially important role in the control of the stem cell properties of MSC.

In this study, we examined the possible roles of Wnt3a in myogenic differentiation, proliferation, and migration of rat MSC (rMSC). The results demonstrated that Wnt3a was sufficient in inducing myogenic differentiation in rMSC by activating the muscular regulatory genes. Thus, to our knowledge, our data suggest that canonical Wnt signaling is sufficient in inducing myogenic lineage commitment in rMSC. In addition, the present study showed that Wnt3a inhibited adipogenic differentiation, but promoted the proliferation and migration of rMSC.

Materials and methods

Isolation and culture of rMSC All of the animal experiments were approved by the Animal Care and Experimentation Committee of Sun Yat-sen University (Guangzhou, China). Adult male Sprague-Dawley rats (60–80 g) were obtained from Sun Yat-sen University Laboratorial Animal Center. The primary MSC were isolated from Sprague-Dawley rats according to the method described by Wakitani *et al* with some modifications[22]. In brief, femora and tibiae of male Sprague-Dawley rats were collected; the adherent soft tissues were carefully removed to ensure that the marrow preparations were not contaminated by myogenic precursors. Both ends of the bones were cut with bone scissors. The bone marrow plugs were hydrostatically expelled from the bones by syringes filled with growth medium. The bone marrow cells were centrifuged and resuspended twice in growth medium. After the cells were resuspended, the cells were introduced into 25 cm^2 tissue culture flasks in 6 mL growth medium. Three days later, the medium was changed and the non-adherent cells were discarded. The medium was completely replaced every 3 d. Approximately 7–10 d after seeding, the culture flasks became nearly confluent and the adherent cells were released from the dishes with 0.25% trypsin (Gibco Laboratories, Grand Island, New York, USA), split 1:2, and seeded into fresh culture flasks. All of the experiments described below were performed using cells from the third to the fifth passage. The cells were cultured in Dulbecco's modified Eagle's medium (DMEM; Gibco Laboratories, Grand Island, New York, USA) and 10% fetal calf serum (FCS; Hyclone, Logan, Utah, USA). Every 3 d the medium was changed once. The cells were grown at 37 °C in a humidified atmosphere with 5% CO_2.

Preparation of Wnt3a-conditioned medium and analysis of the Wnt3a protein The mouse L cells were obtained from the American Type Culture Collection (CRL-2648, Manassas, VA, USA). The cells were cultured in DMEM supplemented with 10% FCS at 37 °C. pGKWnt3a and pGKneo (control) plasmids were generously provided by Prof Shinji TAKADA (Okazaki Institute for Integrative Biosciences, National Institutes of Natural Sciences, Okazaki, Aichi, Japan). pGKWnt3a was constructed by inserting the mouse Wnt3a

cDNA, whose expression was driven by a promoter of rat phosphoglycerokinase gene (PGK promoter) and terminated at a transcriptional terminator sequence of the bovine growth hormone gene, into pGKneo, containing the neomycin phosphotransferase gene (neo) driven by the PGK promoter. The L cells were transfected with pGKWnt3a or pGKneo plasmids by Lipofectamine 2000 according to manufacturer's instruction (Invitrogen, Carlsbad, California, USA). Briefly, the L cells were seed on 35 mm culture plates at a density of 5×10^5 cells per cm^2. Lipofectamine diluted in Opti-MEM (Invitrogen, Carlsbad, California, USA) was applied to the plasmid mixture and the formulation was continued for 25 min. In total, 1 μg pGKWnt3a or pGKneo plasmids with 8 μL Lipofectamine were applied in a final volume of 1.0 mL/well. The transfection media were replaced with growth medium after 4 h of incubation at 37 °C. The cells were selected by G418 (0.4 g/L, Sigma, Saint Louis, Missouri, USA) for 3 weeks and stably transfected clones were then selected. The L cells transfected with pGKWnt3a or pGKneo plasmids were termed L-Wnt3a or control L-cells. The Wnt3a-conditioned medium (Wnt3a-CM) and the control L-conditioned medium (L-CM) were prepared as described previously[23]. Briefly, 1×10^6 L-Wnt3a or L cells were seeded in 100 mm dishes containing DMEM with 10% FCS. After 3 d of culture, the cells were cultured with fresh medium and incubated for 1 more day. Then the medium was collected, centrifuged at 1000×*g* for 10 min, and filtered through a nitrocellulose membrane. The conditioned media were stored at -80 °C until use. The abundance of the Wnt3a protein in Wnt3a-CM and L-CM, as well as in the extracts of L-Wnt3a and control L-cells, was detected by Western blot analysis. The Wnt3a protein in Wnt3a-CM and L-CM was diluted 1:1 in Western blot sampling buffer, containing 20% glycerin, 10% 2-mercaptoethanol, 4% SDS, and bromophenol blue, was boiled for 5 min at 95 °C and frozen at -80 °C until required. The cell lysates were prepared by lysing the cells on ice in Western blot sampling buffer, then boiled for 5 min at 95 °C and frozen at -80 °C until required. The Western blot analysis was performed with a primary rabbit anti-Wnt3a antibody (1:500, Santa Cruz Biotechnology, Santa Cruz, California, USA) and a secondary antirabbit peroxidase antibody (1:3000, Santa Cruz Biotechnology, Santa Cruz, California, USA). Wnt3a-CM was depleted of the Wnt3a protein by incubation with 4 μg/mL rabbit anti-Wnt3a antibody (Santa Cruz Biotechnology, Santa Cruz, California, USA) at 4 °C overnight. The conditioned medium was called Wnt3a-depleted-conditioned medium (Wnt3a depl-CM) and was used to perform antibody blocking experiments.

Flow cytometry (FACS) analysis An analysis of cell surface molecules was performed on passage 3 cultures of rMSC using flow cytometry and the following procedure. The medium was removed from flasks; the cell layers were washed twice with phosphate-buffered saline (PBS) and detached from the flasks by incubation with a solution of 0.25% trypsin for 3–5 min at room temperature. The cells were collected by centrifugation and washed in flow cytometry buffer consisting of 2% bovine serum albumin (BSA) and 0.1% sodium azide in PBS. Then the rMSC were incubated with fluorescein-5-isothiocyanate (FITC)-conjugated monoclonal antibodies, including anti-CD11b, anti-CD29, anti-CD44, and anti-CD45 (Chemicon, Temecula, CA, USA). All incubations with antibodies were performed for 30 min, after which the cells were washed with flow cytometry buffer. The washed cells were pelleted and resuspended in flow cytometry buffer containing 1% paraformaldehyde for 15 min. Non-specific fluorescence was determined using equal aliquots of the cell preparation that were incubated with antimouse monoclonal antibodies. Data were acquired and analyzed on FACSCalibur with CellQuest software (Becton Dickinson, San Jose, CA, USA).

Measurement of rMSC proliferation To study the effect of Wnt3a on rMSC proliferation, rMSC at passage 3 were inoculated on 24-well plates at a density of 1×10^4 cells/cm^2 in the growth medium supplemented with varying concentrations of control L-CM, Wnt3a-CM, or Wnt3a depl-CM. After 96 h, the cells were harvested using trypsin and counted in a hemocytometer. For the determination of 5-bromodeoxyuridine (BrdU) incorporation, the cells were grown in 6-well plates and treated as described earlier. After 72 h, BrdU (Sigma, Saint Louis, Missouri, USA) was added at 5 μg/mL. The cells were then incubated for 4 h and fixed. The detection of BrdU was performed with a mouse anti-BrdU (Sigma, Saint Louis, Missouri, USA), and a secondary anti mouse-cyanine (CY) 3 (Santa Cruz Biotechnology, Santa Cruz, California, USA) was used for visualization. Six areas/well were randomly selected and automatically counted with a computer-connected light microscope. All proliferation assays were performed in triplicate.

Skeletal myogenic differentiation To induce myogenic differentiation, the cells were plated at a density of 5×10^4 cells/mL in 6-well tissue culture plates and allowed to adhere for 24 h at 37 °C, at which time the cells were switched to myogenic medium consisting of DMEM, 2% horse serum, and varying concentrations of control L-CM, Wnt3a-CM, or Wnt3a depl-CM. The medium was changed every 3–4 d and the cells were analyzed for the expression of the muscle-specific markers desmin and myosin heavy chain (MHC) after up to 10 d in culture.

Osteogenic differentiation To induce osteogenic differentiation, the cells were plated at a density of 5×10^4 cells/mL in 6-well tissue culture plates and allowed to adhere for 24 h. Then rMSC were incubated in growth medium

supplemented with 0.01 μmol/L dexamethasone, 10 mmol/L glycerophosphate, and 50 mmol/L L-ascorbic acid-2-phosphate (Sigma, Saint Louis, Missouri, USA). Osteogenic differentiation was observed after 3 weeks by the deposit of a mineralized hydroxyapatite extracellular matrix, as detected by microscopy after staining with 40 mmol/L Alizarin Red S (Sigma, Saint Louis, Missouri, USA).

Adipogenic differentiation To induce adipogenic differentiation, the cells were plated at a density of $5×10^4$ cells/mL in 6-well tissue culture plates and allowed to adhere for 24 h. Then the cells were switched to adipogenic medium (DMEM, 10% FBS, 1 μmol/L dexamethasone, 0.5 mmol/L methylisobutylxanthine, and 10 μg/mL insulin; Sigma, Saint Louis, Missouri, USA) for 21 d and analyzed by Oil Red O (Sigma, Saint Louis, Missouri, USA) staining. To study the effect of Wnt3a on rMSC adipogenesis, the cells were seeded at a density of $5×10^4$ cells/mL in 6-well tissue culture plates and cultured for 3 weeks in adipogenic medium, supplemented with different concentrations of control L-CM, Wnt3a-CM, or Wnt3a depl-CM. The medium was refreshed every 3–4 d and lipid formation was detected after 21 d by Oil Red O staining. The adipocytes were washed with PBS, fixed for 30 min in formol (3.7% formalin plus $CaCl_2.3.2H_2O$), and stained for 10 min in freshly-filtered Oil Red O solution (stock: 500 mg Oil Red O, 99 mL isopropanol, 1 mL water; stain: 42 mL stock plus 28 mL water). Oil Red O staining was quantified by extraction with 4% Igepal (Sigma, Saint Louis, Missouri, USA) in isopropanol for 15 min and measurement of absorbance at 520 nm. Values represent the mean±SD.

Transwell migration assay Transwell migration assays were performed with 6.5 mm diameter, Falcon cell culture inserts (8 μm pore size; Becton Dickinson, San Jose, California, USA) and 24-well cell culture plates. rMSC were trypsinized, resuspended in serum-free DMEM, and transferred to the upper chamber ($5×10^4$ cells resuspended in 1.0 mL pre-equilibrated DMEM). An equal volume maintenance medium supplemented with varying concentrations of control L-CM, Wnt3a-CM, or Wnt3a depl-CM was added to the lower chamber. The cells were allowed to migrate for 24 h in a humidified CO_2 incubator at 37 °C. Following incubation, the media were aspirated, and the cells remaining on the upper surface of the filter were removed with a cotton swab; the cells that had migrated to the lower surface were stained with hematoxylin for 30 min. The average numbers of migrated cells were determined by counting the cells in 6 random high-power fields (×200). The transwell assays for each condition were performed in triplicate and representative results are shown.

Wound healing assay For the wounding healing assay, rMSC were plated in 6-well tissue culture plates and allowed to grow to a confluency of 70%–80%. The experimental wounds were made by dragging pipette tips across the cell culture. The cultures were then rinsed with PBS and replaced with fresh maintenance medium supplemented with varying concentrations of control L-CM, Wnt3a-CM, or Wnt3a depl-CM. The wound healing at approximately the same fields was recorded under a bright field at selected time-points. The wound gap was measured, and the percentage of wound repair was determined for each time-point. All treatments were assessed in triplicate.

Immunofluorescence analysis For the immunofluorescence analysis, the cells grown on glass coverslips were fixed in methanol/acetone (1:1, *v/v*) for 10 min at room temperature. Blocking was carried out in 3% BSA in PBS for 30 min and the primary antibody was diluted at 1:50 (β-catenin, Cell Signaling Technology, Danvers, Massachusetts, USA) and 1:200 (desmin and MHC; Santa Cruz Biotechnology, Santa Cruz, California, USA) in a solution containing 3% BSA. Incubation was carried out at room temperature for 1 h or at 4 °C overnight. After 3 washes in PBS, the secondary antibody (CY3-conjugated goat antirabbit, FITC-conjugated goat antirabbit, Santa Cruz Biotechnology, Santa Cruz, California, USA) was used at a 1:200 dilution in 3% BSA, and the incubation lasted for 1 h at room temperature. The nuclear localization of immunostaining was confirmed by counterstaining with 4',6-diamidino-2-phenylindole (DAPI, Sigma, Saint Louis, Missouri, USA) at a 1:5000 dilution in PBS. The immunofluorescence images were recorded using an Olympus immunofluorescence microscope (Olympus Optical Company, Ltd, Tokyo, Japan). The percentages of β-catenin-, desmin-, and MHC-positive cells were calculated from the ratio of positive cells to the total cells counted. Six random fields at 20-fold magnification were examined under the microscope at the indicated time-points. Values represent the mean±SD.

RT-PCR Total RNA was extracted from the cells at the indicated time-points using Trizol reagent (Invitrogen, Carlsbad, California, USA) and treated with RNase-free DNase (Fermentas, Hanover, Maryland, USA) to remove any contaminating genomic DNA according to the manufacturer's protocol. One microgram of total cellular RNA was reversely transcribed using the Revert Aid TM H Minus First Strand Synthesis Kit (Fermentas, Hanover, Maryland, USA) for 60 min at 42 °C. cDNA was heated at 70 °C for 10 min. The first-strand synthesized cDNA was used directly for PCR amplification. Each PCR reaction was carried out in 25 μL mixture. The primer sequences used for the PCR amplification were designed based on published cDNA sequences and are as follows: 5'-GGC TTT CAA CCA TCT CAT TC-3' and 5'-GTT GGT CAG AAG TCC CAT TAC-3' for Pax3, generating a 343 bp fragment; 5'-TTC GGG AAG AAA GAG GAC G-3' and 5'-ATG GTT GAT GGC GGA AGG-3' for Pax7, gener-

ating a 512 bp fragment; 5'-CTA CAG CGG CGA CTC AGA CG-3' and 5'-TTG GGG CCG GAT GTA GGA-3' for MyoD, generating a 563 bp fragment[24]; 5'-TTA GAA GTG GCA GAG GGC TC-3' and 5'-AGG TGC GCA GGA AAT CCG CA-3' for Myf4, generating a 475 bp fragment[25]; 5'-GAG CCA AGA GTA GCA GCC TTC G-3' and 5'-GTT CTT TCG GGA CCA GAC AGG G-3' for Myf5, generating a 440 bp fragment[26]; 5'-ACT ACC CAC CGT CCA TTC AC-3' and 5'-TCG GGG CAC TCA CTG TCT CT-3' for myogenin, generating a 233 bp fragment[24]; 5'-CTC AGG CTT CAA GAT TTG GTG G-3' and 5'-TTG TGC CTC TCT TCG GTC ATT C-3' for MHC, generating a 265 bp fragment; 5'-GCC TTG CTG TGG GGA TGT CT-3' and 5'-CGA AAC TGG CAC CCT TGA AAA AT-3' for peroxisome proliferator-activated receptor gamma (PPARγ), generating a 355 bp fragment; and 5'-GGC GGG AAC GCA ACA ACA-3' and 5'-GAG ATC CAG CGA CCC TAA ACC A-3' for CCAAT/enhancer-binding protein alpha (C/EBPα), generating a 292 bp fragment. To control the amount of RNA in the different samples, the expression of GADPH was amplified with the following primers: 5'-ACC ACA GTC CAT GCC ATC AC-3' and 5'-TCC ACC ACC CTG TTG CTG TA-3' and generating a 451 bp fragment[27]. All the primers were synthesized by Saibaisheng (Beijing, China). The amplification products were electrophoresed on 1.5% agarose gels and visualized by ethidium bromide staining followed by UV light illumination.

Statistical analysis All data were presented as mean±SD. The statistical differences among 3 or more groups were determined by ANOVA, followed by a Dunnett's *post-hoc* test of all groups versus the respective control group. The statistical differences between 2 groups were performed by Student's *t*-test. A value of $P<0.05$ was considered statistically significant.
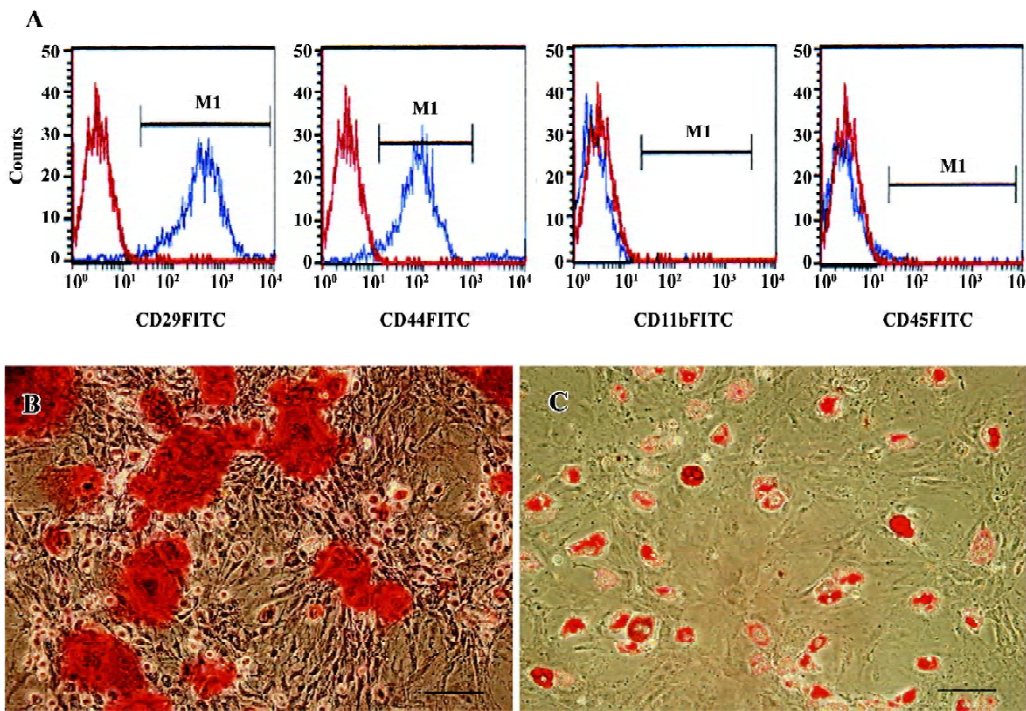
Results

Characterization of rMSC in culture To characterize rMSC, we first performed FACS to detect the immunophenotype of isolated rMSC at passage 3. The results showed that rMSC expressed CD29 (β1-integrin) and CD44. The positive ratio of CD29 and CD44 were 97.8% and 95.1%, respectively. In contrast, rMSC did not express CD11b (Mac-1) and CD45, which are markers of hematopoietic stem cells (Figure 1A). Furthermore, we induced cell differentiation of isolated rMSC according to published protocols[2]. In the presence of an osteogenic stimulus, rMSC developed into osteoblastic cells, as judged by their ability to mineralize the extracellular matrix (Figure 1B). After exposure to an adipogenic stimulus, the cells displayed an adipocyte phenotype, as shown by the accumulation of neutral lipid droplets in the cytoplasm (Figure 1C). These results confirm that the iso-

lated cells exhibit the previously reported properties of MSC[2].

Activating Wnt signaling induces β-catenin nuclear translocation in rMSC To explore the role of Wnt3a signaling in the proliferation, differentiation, and migration of rMSC, Wnt3a-CM were prepared and the presence of the Wnt3a protein in Wnt3a-CM were confirmed by Western blot analysis (Figure 2C). To determine whether Wnt3a-CM activate the canonical pathway of Wnt signaling in rMSC, rMSC were exposed to Wnt3a-CM and changes in β-catenin localization were detected by fluorescent immunocytochemistry. The results showed that β-catenin was detected in the cytoplasm and at peripheral sites of cell-cell contact after exposure to control conditioned medium. In comparison, β-catenin was predominantly identified in the nucleus of cells, determined by colocalization with nuclear staining by DAPI after rMSC were cultured in Wnt3a-CM for 24 h (Figure 2A). These observations were quantified, and the result showed that Wnt3a-induced nuclear translocation was dose-dependent and increased from 0% of cells with nuclear β-catenin in L-CM-treated cells to 84.5%±4.37% in the 50% Wnt3a-CM-treated cells ($P<0.001$; Figure 2B). To determine whether the effect of Wnt3a-CM on β-catenin nuclear translocation in rMSC was indeed due to the Wnt3a protein, we detected β-catenin localization in rMSC after the cells were exposed to Wnt3a-CM that had first been blocked from Wnt3a using a Wnt3a antibody. As shown in Figure 2, the depletion of Wnt3a completely abolished the ability of Wnt3a-CM to induce β-catenin nuclear translocation in rMSC. These results demonstrate that Wnt3a possesses the ability to induce β-catenin nuclear translocation and activate the Wnt pathway in rMSC.

Effects of Wnt3a on rMSC proliferation To analyze the effect of Wnt3a-CM on the proliferation of rMSC, we cultured these cells in growth medium containing differentiation concentrations of Wnt3a-CM or L-CM. The cells were harvested using trypsin and counted in a hemocytometer at the indicated time-points. Compared with the control L-CM, Wnt3a led to a significant increase in the number of rMSC, both at 25% ($3.04\times10^4\pm0.43\times10^4$ *vs* $3.89\times10^4\pm0.31\times10^4$, $P<0.05$) and 50% conditioned medium ($3.16\times10^4\pm0.39\times10^4$ *vs* $4.14\times10^4\pm0.37\times10^4$, $P<0.05$) after being cultured for 5 d (Figure 3A). To test whether the effect of Wnt3a-CM on the proliferation of rMSC was specific to Wnt3a, rMSC were cultured in growth medium containing different concentrations of Wnt3a depl-CM. The result showed that the depletion of Wnt3a significantly reduced the ability of Wnt3a-CM to stimulate the proliferation of rMSC after 5 d of treatment (25%, $2.95\times10^4\pm0.39\times10^4$ *vs* $3.89\times10^4\pm0.31\times10^4$, $P<0.05$; 50%, $3.05\times10^4\pm0.42\times10^4$ *vs* $4.14\times10^4\pm0.37\times10^4$, $P<0.05$; Figure 3A). These results suggest that Wnt3a is mitogenic to rMSC.

To further evaluate the Wnt effect on rMSC proliferation,

Figure 1. Characterization of isolated rMSC. (A) FACS analysis of rMSC. Result shows that rMSC expressed CD29 and CD44, but not CD11b and CD45. (B) Osteogenic differentiation of rMSC. RMSC were cultured for 3 weeks with osteogenic induction medium, and calcium deposits were visualized by Alizarin Red S staining. (C) Adipogenic differentiation of rMSC. RMSC were cultured for 3 weeks in adipogenic induction medium. Lipid vacuoles were visualized by Oil Red O staining. Results are representative graphs of 3 independent experiments. Scale bar: 100 μm (original magnification ×200).
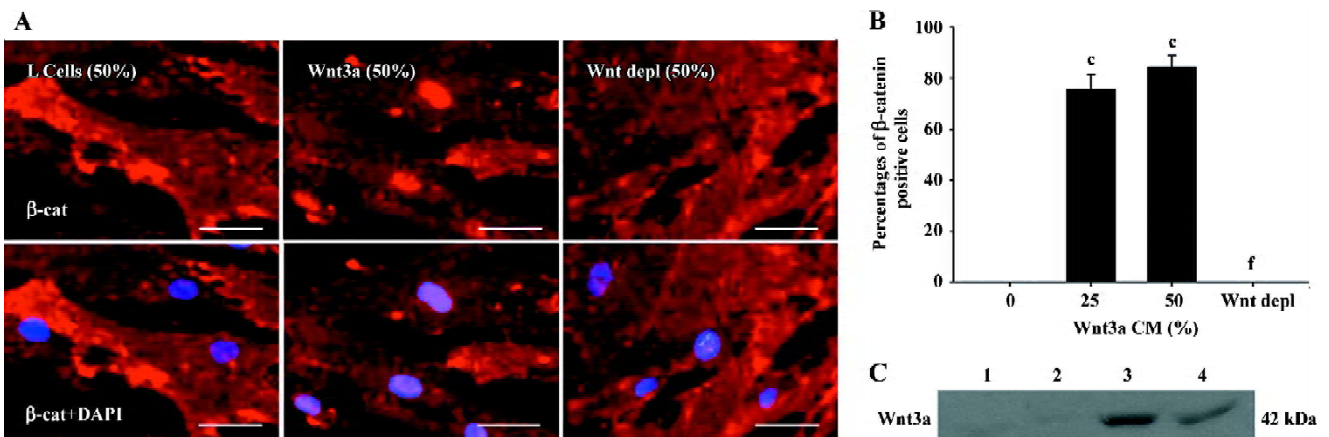
Figure 2. Immunofluorescence analysis of the subcelluar localization of β-catenin in rMSC. (A) rMSC were exposed to 50% control conditioned medium (L-cells), Wnt3a-CM (Wnt3a), or Wnt depl-CM (Wnt depl) for 24 h. Changes in β-catenin localization were detected by an anti-β-catenin antibody. β-catenin was predominantly localized in the nucleus of cells after rMSC were cultured in Wnt3a-CM for 24 h compared with the cells incubated with control conditioned medium. Scale bar: 50 μm (Original magnification ×400). (B) Dose-dependence of Wnt3a-induced β-catenin translocation in rMSC. No effect was observed in the cells exposed to L-CM and Wnt depl-CM at the different concentrations tested. $n=3$. Mean±SD. [c]$P<0.01$ *vs* control L-CM group. [f]$P<0.01$ *vs* Wnt3a-CM group.(C)Presence of Wnt3a in Wnt3a-CM. Western blot analysis of the Wnt3a protein was conducted on the cell extract of L-Wnt3a cells (lane 3) and Wnt3a-CM (lane 4) compared with control L cells (lane 1) and L-CM (lane 2). The 42 kDa Wnt3a protein bands were present in both the cell extracts of L-Wnt3a and Wnt3a-CM.

we measured the effect of Wnt3a-CM on BrdU incorporation into rMSC. The incorporated BrdU was detected by using a monoclonal antibody against BrdU. The proportion of BrdU-positive cells increased about 1.42- and 1.75-fold in the Wnt3a-treated cells compared with the control cells (25%, 12.5%±2.18% *vs* 17.8%±2.36%, $P<0.05$; 50%, 11.8%±2.49% *vs* 20.6%±4.45%, $P<0.05$; Figure 3B,3C). After culturing rMSC in Wnt3a depl-CM, the proportion of BrdU-positive cells reduced to 10.8%±2.37% and 13.1%±3.04% ($P<0.05$; Figure 3B,3C). These results further demonstrate that Wnt signal-
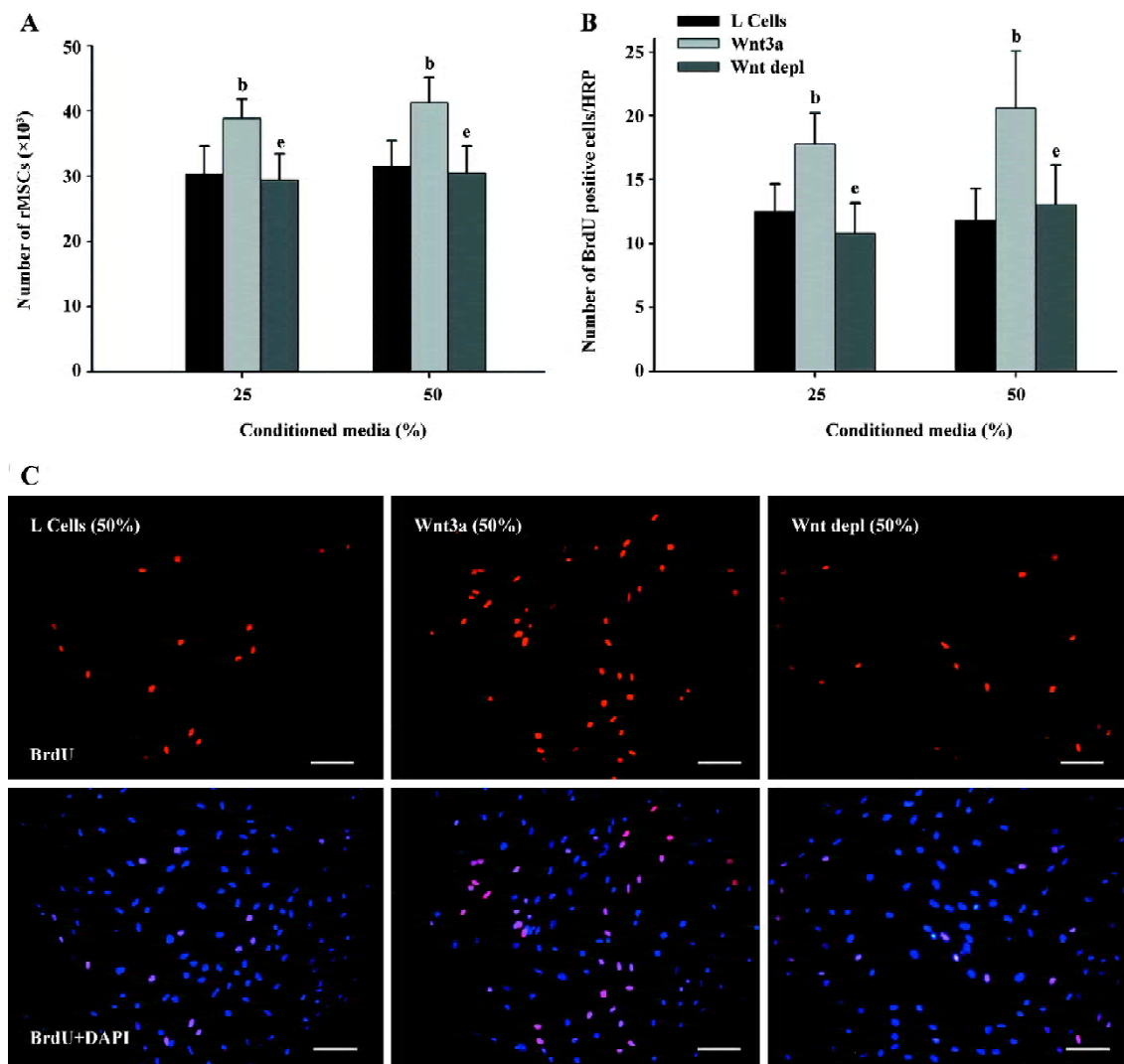
Figure 3. Effect of Wnt3a on rMSC proliferation. (A) rMSC at passage 3 were inoculated on 24-well plates at a density of 1×10^4 cells/cm^2 in the maintenance medium supplemented with varying concentrations of control L-CM (L cells), Wnt3a-CM (Wnt3a), or Wnt3a depl-CM (Wnt depl). After 96 h, the cells were harvested using trypsin and counted in a hemocytometer. Compared with the control L-CM and Wnt3a depl-CM, Wnt3a-CM led to a statistically significant increase in the number of rMSC in a dose-dependent fashion. $n=3$. Mean±SD. $^bP<0.05$ *vs* control L-CM group. $^eP<0.05$ *vs* Wnt3a-CM group. (B) Effect of Wnt3a-CM on BrdU incorporation of rMSC. RMSC at passage 3 were inoculated on 6-well plates at a density of 1×10^4 cells/cm^2 in the maintenance medium supplemented with 50% control L-CM (L cells), Wnt3a-CM (Wnt3a), or Wnt3a depl-CM (Wnt depl). After 72 h, BrdU was added at 5 μg/mL. Cells were incubated for 4 h and then fixed for immunofluorescence analysis. Cell nuclei were stained with DAPI. Cells containing BrdU incorporated into the nucleus were scored as BrdU-positive cells. $n=3$. Mean±SD. $^bP<0.05$ *vs* control L-CM group. $^eP<0.05$ *vs* Wnt3a-CM group. (C) Immunofluorescence analysis of BrdU in rMSC. Results are representative graphs of 3 independent experiments. Scale bar: 100 μm (original magnification ×200).

ing is capable of promoting the proliferation of rMSC.

Wnt3a-expanded rMSC retain their pluripotency To demonstrate that rMSC after Wnt3a treatment maintain their pluripotency for differentiation, we expanded rMSC in proliferation medium with or without Wnt3a-CM and compared their osteogenic and adipogenic differentiation *in vitro*. After cultivation in the Wnt3a-CM for 6 d, rMSC were replated

and induced for osteogenic or adipogenic differentiation in the absence of Wnt3a. When Wnt3a-expanded rMSC were cultured in the osteogenic medium, the osteogenic differentiation of these cells was similar to that of the control cells (Figure 4). Similarly, when Wnt3a-expanded rMSC were induced for adipogenic differentiation, an accumulation of fat vacuoles in the cytoplasm were observed in these cells as
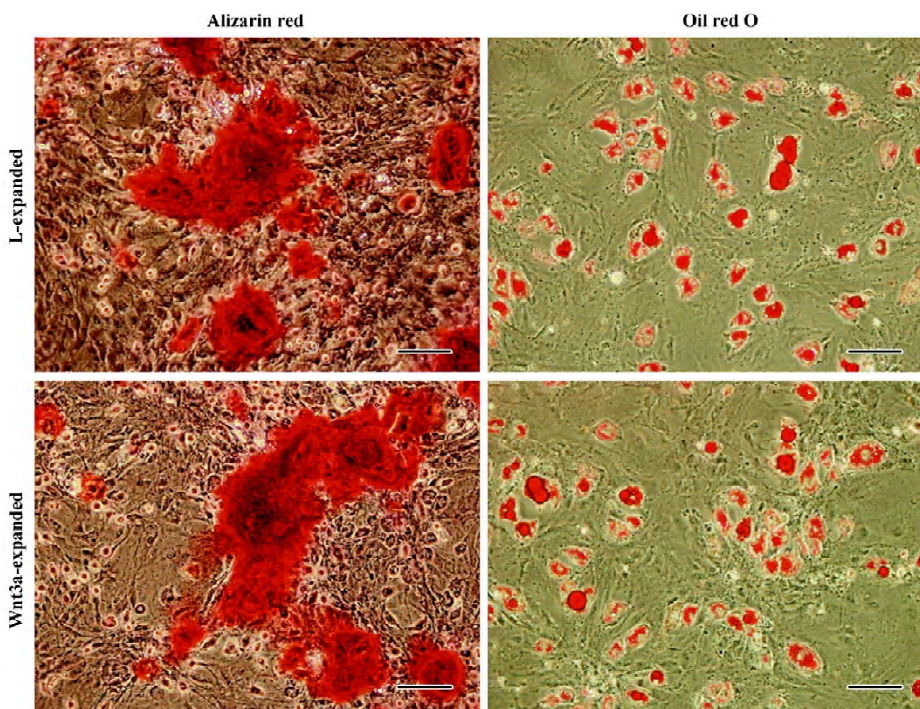
Figure 4. Wnt3a-expanded rMSC retain their pluripotency. After cultivation in proliferation medium with (Wnt3a-expanded) or without (L-expanded) 50% Wnt3a-CM for 6 d, rMSC were replated and induced for osteogenic or adipogenic differentiation for 3 weeks. Osteogenic differentiation of rMSC was detected by alizarin red staining. Adipogenic differentiation of rMSC was stained by Oil Red O. Results are representative graphs of 3 independent experiments. Scale bar: 100 μm (original magnification ×200).

well as the control cells (Figure 4). These results suggest that Wnt3a-expanded rMSC retain their pluripotency.
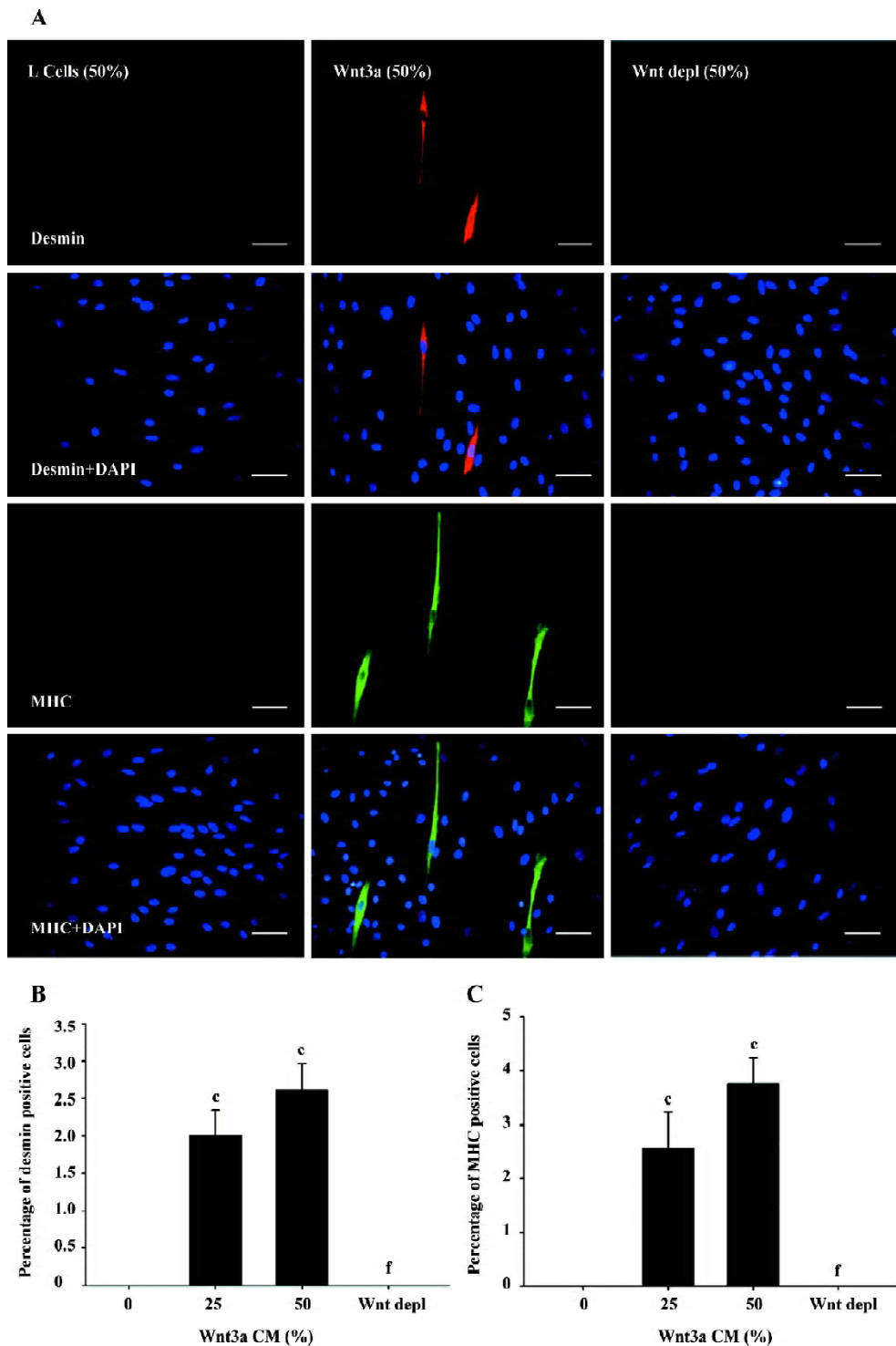
Wnt3a induces the myogenic differentiation of rMSC
Wnt signaling has been shown to play an important role in the induction of myogenesis during embryonic development. In order to investigate a possible role for Wnt3a in inducing the myogenic differentiation of rMSC, we cultured rMSC in myogenic medium supplemented with Wnt3a-CM. The treated cells were observed by phase-contrast microscopy every day and further analyzed by immunofluorescence with antibodies against desmin and MHC. After 7–10 d, we observed that the morphology of a few Wnt3a-treated cells changed from a fibroblast-like phenotype to elongated mononucleated, myotubes-like shape. To further confirm the myogenic nature of the mononucleated cells observed by phase-contrast microscopy, immunofluorescence was examined in Wnt3a-treated rMSC with antibodies that detected desmin and MHC (Figure 5A). As shown in Figure 5B, approximately 2%–3% of all rMSC stained positive for desmin after 25% and 50% Wnt3a-CM treatment. The positive ratio for MHC was 2.57%±0.66% and 3.76%±0.48% in the presence of 25% and 50% Wnt3a-CM (Figure 5C). On the other hand, no obvious morphological changes, desmin-, or MHC-positive cells were observed in the L-CM treated cells (Figure 5A).

To determine whether the role of Wnt3a-CM in inducing the myogenic differentiation of rMSC was specific to Wnt3a, we performed a myogenic differentiation experiment in rMSC

after the cells were exposed to Wnt3a-CM that had been depleted of the Wnt3a protein by adding the Wnt3a antibody. As shown in Figure 5A, there were no desmin- or MHC-positive cells observed in Wnt3a depl-CM treated cells. Therefore, the depletion of Wnt3a completely abolished the ability of Wnt3a-CM to induce myogenic differentiation in rMSC. These findings suggest that the role of Wnt3a-CM on myogenic differentiation in rMSC is specific to Wnt3a.

To examine whether the myogenic differentiation of Wnt3a-treated rMSC was acquired through a cascade of molecular events reminiscent of embryonic myogenesis, a systematic study of the temporal expression pattern of myogenic differentiation genes during the treatment of rMSC with Wnt3a was examined by RT-PCR. As shown in Figure 6, changes in the expression profiles of myogenic differentiation genes were observed after Wnt3a treatment. RMSC only expressed Pax3, but not Pax7 and other myogenic regulatory factors, including MyoD, Myf4, Myf5, and myogenin before Wnt3a treatment. Pax7 was activated at first after 2 d Wnt3a treatment. Following the expression of Pax7, the expression of MyoD and Myf5 were observed at 4 d treatment. The expression of Myf4, myogenin was found after 6 d treatment. MHC was also weakly expressed at d 6. None of these transcription factors, except Pax3, was detected in rMSC treated with L-CM (data not shown). These results demonstrate that Wnt3a induces myogenic differentiation of rMSC through triggering the expression of myogenic regulatory factors.

A

B

C

Figure 5. Wnt3a induces myogenic differentiation in rMSC (A) rMSC were plated at a density of 5×10^4 cells/mL in 6-well tissue culture plates and cultured in myogenic medium consisting of DMEM, 2% horse serum, 50% L-CM (L cells), Wnt3a-CM (Wnt3a), or Wnt3a depl-CM (Wnt depl). Cells were stained for desmin and MHC after 10 d in culture. Cell nuclei were stained with DAPI. The expression of desmin and MHC was activated after the cells were exposed to Wnt3a-CM. No desmin- or MHC-positive cells were observed in the control group and Wnt3a depl-CM group. Results are representative graphs of 3 independent experiments. Scale bar: 100 µm (original magnification ×200). (B, C) quantitative measurement of the percentage of desmin- and MHC-positive cells after Wnt3a treatment. The percentages of desmin- and MHC-positive cells were calculated from the ratio of positive cells to total cells counted. Six random fields at 20-fold magnification were examined under the microscope at the indicated time point. Expression of desmin and MHC was induced by Wnt3a in a dose-dependent fashion. No desmin- or MHC-positive cells were observed in the cells exposed to control L-CM and Wnt3a depl-CM. *n*=3. Mean±SD. [c]*P*<0.01 *vs* control L-CM group. [f]*P*<0.01 *vs* Wnt3a-CM group.

Effect of Wnt3a on adipogenic differentiation of rMSC
Recently, the Wnt signaling pathway has been shown to inhibit adipogenesis in 3T3-L1 pre-adipogenic cells and human MSC[28,29]. Therefore, we examined whether Wnt3a signaling had an inhibitory effect on rMSC adipogenesis. For

this analysis, rMSC were incubated in adipogenic differentiation medium supplemented with Wnt3a-CM for 3 weeks. The adipogenic differentiation was evidenced by the positive Oil Red O staining of lipid droplets presented in the cytoplasm of the cells. As shown in Figure 7A, the control
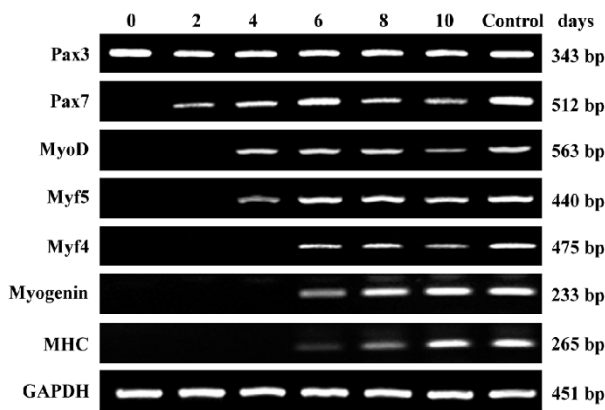
Figure 6. Temporal pattern of expression of myogenic differentiation genes activated during the treatment of rMSC with Wnt3a. Total RNA was isolated from rMSC cultured in myogenic differentiation medium supplemented with 50% Wnt3a-CM every 2 d for 10 d. RT–PCR was performed with primers specific for Pax3, Pax7, MyoD, Myf5, Myf4, myogenin and MHC. GADPH was used as an internal control. Fetal Sprague-Dawley rat skeletal muscle cells (control) were used as positive controls. All experiments are representative of 3 replicates.

cells accumulated a lot of lipid droplets after the induction of adipogenesis. In contrast, the accumulation of lipid droplets was dramatically blocked in Wnt3a-treated rMSC. The inhibitory effect of Wnt3a was dose-dependent. Lipid formation in the control cells and Wnt3a-treated rMSC was quantified and the result showed that the accumulation of lipid decreased by 34.9% and 46.8% in the presence of 25% and 50% Wnt3a-CM compared with the control cells (25%, 0.96±0.11 *vs* 0.62±0.04, $P<0.01$; 50%, 0.95±0.08 *vs* 0.51±0.04, $P<0.01$; Figure 7B). To determine whether the effect of Wnt3a-CM on adipogenic differentiation in rMSC was due to Wnt3a, rMSC were incubated in adipogenic differentiation medium supplemented with 25% and 50% Wnt3a depl-CM. The results showed that the depletion of Wnt3a eliminated the inhibitory role of Wnt3a-CM on adipogenic differentiation in rMSC (25%, 0.87±0.09 *vs* 0.62±0.04, $P<0.05$; 50%, 0.93± 0.07 *vs* 0.51±0.04, $P<0.01$; Figure 7A, 7B). These findings suggest that the role of Wnt3a-CM on the adipogenic differentiation in rMSC is specific to Wnt3a.

To further investigate the mechanism involved in the inhibition of adipogenesis, we examined the effect of Wnt3a
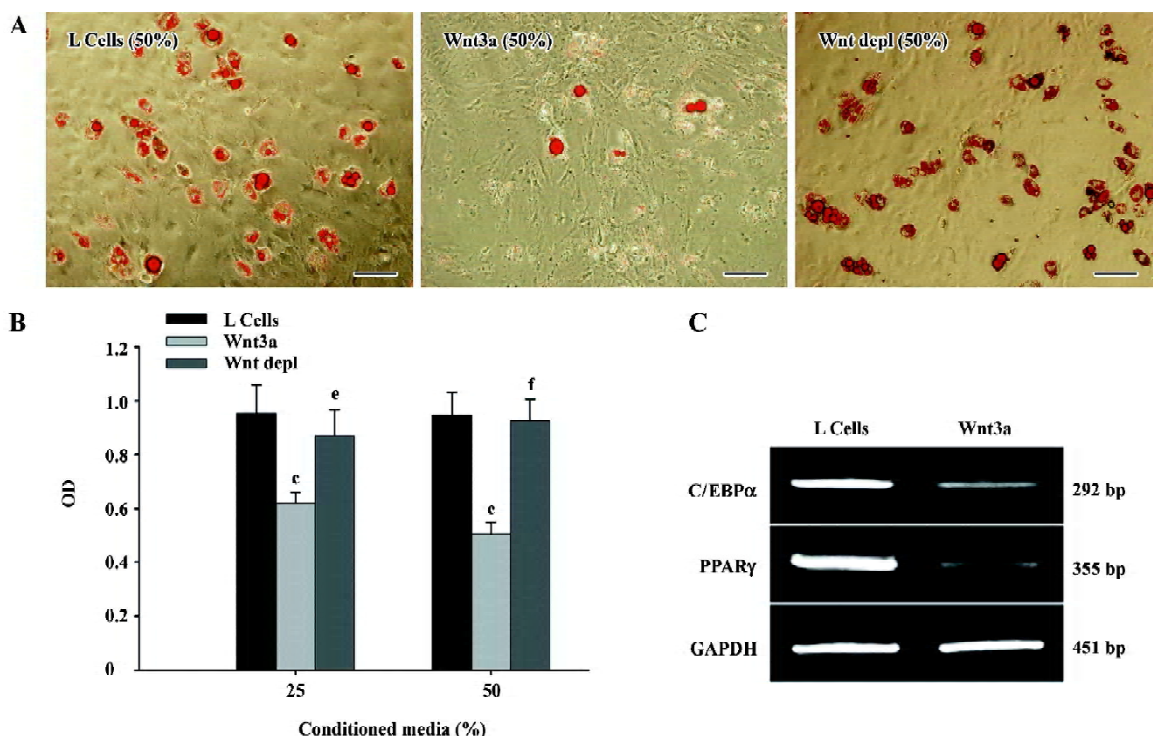
Figure 7. Effect of Wnt3a on the adipogenic differentiation of rMSC. (A) rMSC were cultured in adipogenic induction medium supplemented with L-CM (L cells), Wnt3a-CM (Wnt3a), or Wnt3a depl-CM (Wnt depl) for 3 weeks and stained with Oil Red O. Scale bar: 100 μm (original magnification ×200). (B) Quantification of lipid formation in rMSC after Wnt3a treatment. Inhibitory effect of Wnt3a on adipogenesis in rMSC was dose dependent. *n*=3. Mean±SD. [c]$P<0.01$ *vs* control L-CM group; [e]$P<0.05$, [f]$P<0.01$ *vs* Wnt3a-CM group. (C) Semiquantitative RT–PCR analysis of the expression of C/EBPα and PPARγ. RNA was isolated from rMSC cultured in adipogenic induction medium supplemented with 50% L-CM (L cells) or Wnt3a-CM (Wnt3a) for 3 weeks. GADPH was used as an internal control. Results are representative graphs of 3 independent experiments.

on expression of C/EBPα and PPARγ by RT-PCR. C/EBPα and PPARγ were the essential transcriptional activators and markers of the terminal differentiation of adipogenesis. Compared with the control cells, the expression of both C/EBPα and PPARγ was downregulated in rMSC after Wnt3a treatment (Figure 7C). These data demonstrate that Wnt signaling has an inhibitory effect on the adipogenic differentiation of rMSC.

Effect of Wnt3a on the migration of rMSC Some therapeutic approaches have demonstrated that MSC are able to regenerate injured tissues when applied from different sites of application. The molecular mechanisms involved in the control of the migration of MSC are widely unknown. Since the Wnt signaling pathway was involved in the metastasis of many kinds of cancer cells, we first conducted transwell migration assays to investigate whether Wnt3a signaling could function as a chemoattractant to mesenchymal stem cells. As shown in Figure 8A, the presence of Wnt3a significantly increased cell migration. In fact, the average migrated cell number of rMSC increased 1.86- and 2.41-fold in the presence of 25% and 50% Wnt3a-CM compared with the controls (25%, 37.6±4.17 *vs* 70.2±13.03, $P<0.05$; 50%, 35.7±7.24 *vs* 86.3±11.60, $P<0.01$; Figure 8B). Compared with the Wnt3a-CM group, the average migrated cell number of rMSC reduced to 32.3±5.38 and 38.5±6.14 in 25% and 50% Wnt3a depl-CM treated groups (25%: $P<0.05$; 50%: $P<0.01$; Figure 8). These results demonstrate that Wnt3a signaling is strongly chemotactic for rMSC.

We next conducted a wound healing assay to determine whether Wnt3a could promote rMSC migration. The wound healing experiment is one of the most commonly used methods to assess cell adhesion and migration under *in vitro* conditions. As shown in Figure 9A, the ability of the cells to migrate was significantly enhanced when they were treated with Wnt3a-CM as compared with those treated with control media. The stimulatory effect of Wnt3a on the migration of rMSC was dose-dependent (Figure 9B). The specificity of the treatment was shown by the reduction in the migration of cells treated with Wnt3a-CM that had been depleted of Wnt3a using the Wnt3a antibody (Figure 9A,9B). The transwell migration and wound healing assays for each condition were performed in triplicate. Taken together, these findings suggest that Wnt3a is a significant factor in regulating the migration of rMSCs *in vitro*.

Discussion

Wnt signals are involved in multiple developmental processes, including differentiation, proliferation, and migration of progenitor cells in the developing embryo. In this study, we evaluated the effects of Wnt3a signaling on the differentiation, proliferation, and migration of rMSC *in vitro*. The results showed that the activation of the canonical Wnt pathway induced myogenic differentiation of rMSC and inhibited their adipogenic differentiation. Furthermore, Wnt3a signaling had the ability to promote rMSC to expand and regulate the migration of rMSC *in vitro*. The specificity of the effects was demonstrated by the ability of a Wnt3a antibody to block the effects of Wnt3a. These results suggest that Wnt signaling play important roles in the regulation of the proliferation, differentiation, and migration of rMSC.

Because MSC have the ability to differentiate into numerous mesenchymal tissue lineages, there has been much interest in these cells and their potential application in cytotherapy and gene therapy. How to rapidly expand MSC using simple methods is an attractive characteristic of the cells and it has been the subject of much investigation. Recent experiments have suggested that Wnt signaling has the capacity to promote self-renewal in various tissue stem cells, including intestinal stem cells, skin stem cells, neural stem cells, and hematopoietic stem cells *in vitro* and *in vivo*[30–33]. In the present study, we demonstrated that Wnt3a could promote the proliferation of rMSC and that Wnt3a-expanded cells preserve their multipotency. These findings indicate that Wnt signaling has a mitogenic effect on rMSC. Thus, our study provides evidence that the activation of canonical Wnt signaling by Wnt3a is useful for expanding MSC *in vitro*.

A crucial role of Wnt signalling for skeletal myogenesis has been demonstrated in embryo development[14,15,34]. It has been shown that either Wnt1 or Wnt3a in combination with Sonic hedgehog is sufficient for activating skeletal muscle-specific genes, such as MyoD and Myf5, in the paraxial mesoderm in coculture experiments[14]. Wnt derived from axial structures (neural tube and notochord) preferentially activate myogenesis through a Myf5-dependent pathway, while Wnt derived from dorsal ectoderm preferentially activate myogenesis through a MyoD-dependent pathway[15]. Other studies have shown that the ectopical implantation of Wnt3a-expressing fibroblasts leads to increased Pax-3 expression in adjacent somites[34]. Wnt3a has also been shown to activate Pax3 and MyoD expressions and results in the induction of myogenesis in P19 embryonal carcinoma cells[35].

At present time, there is no study available on the role of Wnt3a in the myogenic differentiation of adult stem cells. To our knowledge, this study provides the experimental evidence that Wnt3a can induce the myogenesis of rMSC. Nevertheless, the efficiency of this induction was low. This suggests that the induction conditions need to be further optimized. In addition, it is possible that other molecules,

A

B
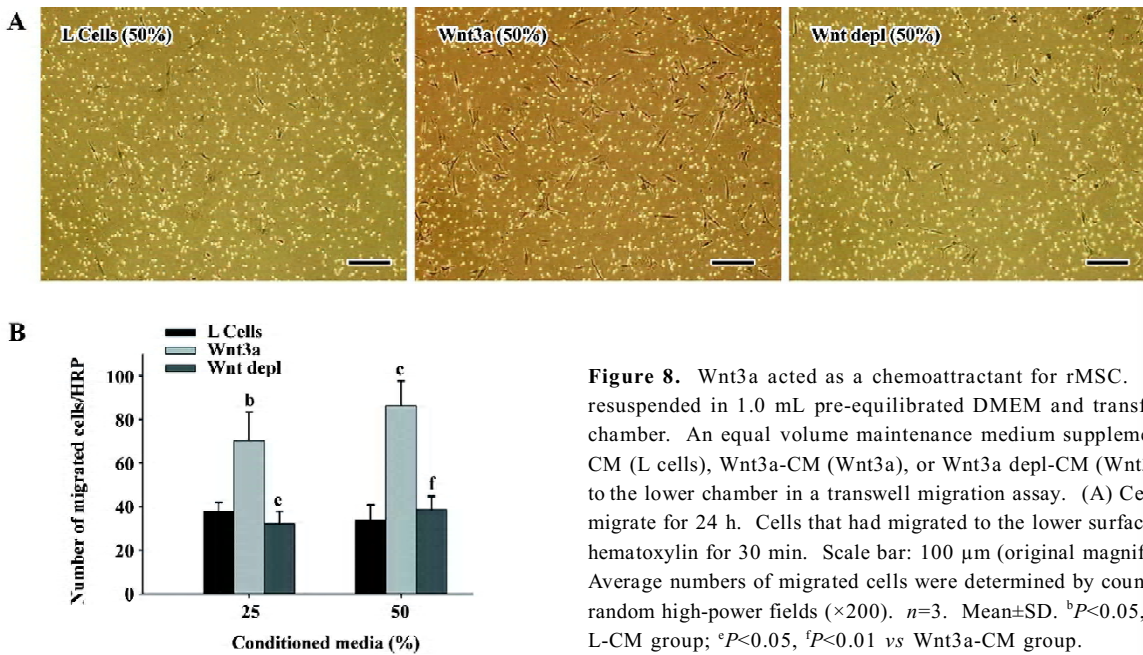
Figure 8. Wnt3a acted as a chemoattractant for rMSC. 5×10^4 rMSC were resuspended in 1.0 mL pre-equilibrated DMEM and transferred to the upper chamber. An equal volume maintenance medium supplemented with 50% L-CM (L cells), Wnt3a-CM (Wnt3a), or Wnt3a depl-CM (Wnt3a depl) was added to the lower chamber in a transwell migration assay. (A) Cells were allowed to migrate for 24 h. Cells that had migrated to the lower surface were stained with hematoxylin for 30 min. Scale bar: 100 µm (original magnification ×200). (B) Average numbers of migrated cells were determined by counting the cells in 10 random high-power fields (×200). *n*=3. Mean±SD. [b]$P<0.05$, [c]$P<0.01$ *vs* control L-CM group; [e]$P<0.05$, [f]$P<0.01$ *vs* Wnt3a-CM group.

A

B
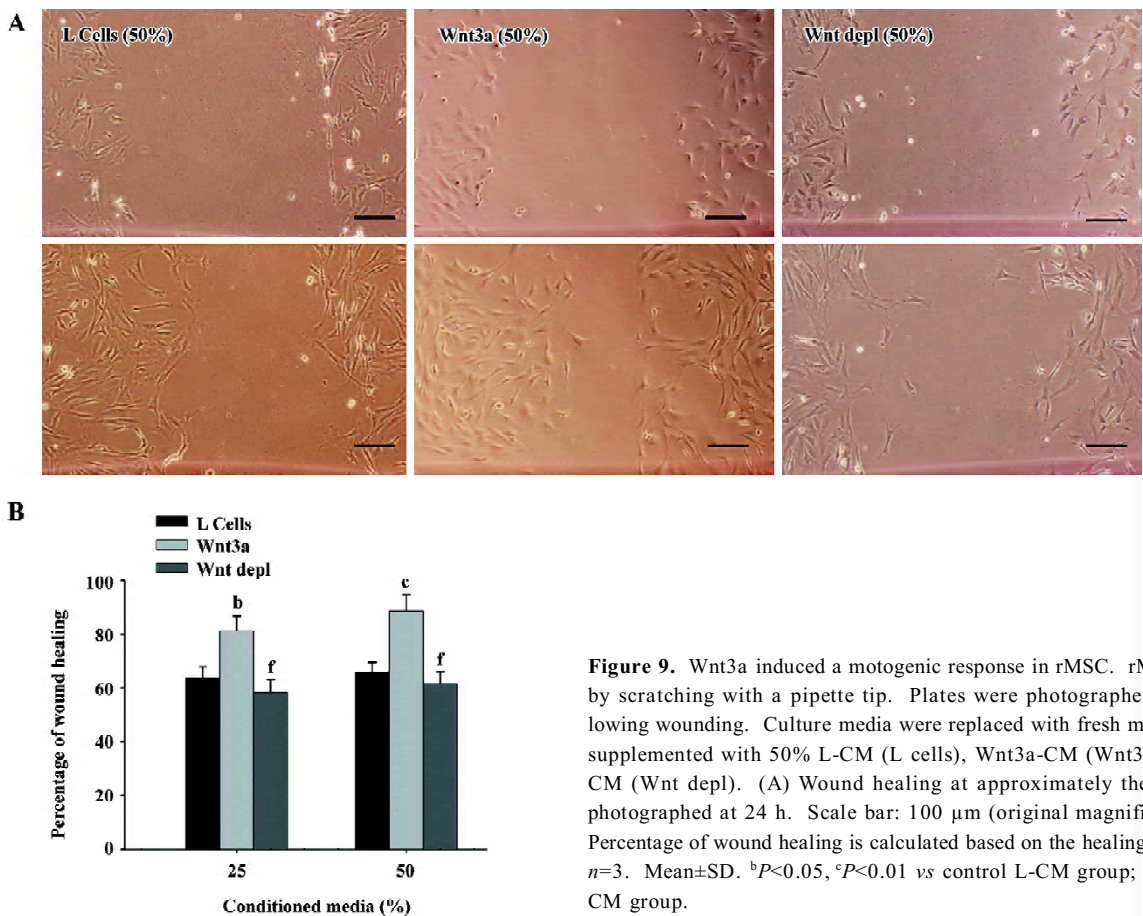
Figure 9. Wnt3a induced a motogenic response in rMSC. rMSC were wounded by scratching with a pipette tip. Plates were photographed immediately following wounding. Culture media were replaced with fresh maintenance medium supplemented with 50% L-CM (L cells), Wnt3a-CM (Wnt3a), or Wnt3a depl-CM (Wnt depl). (A) Wound healing at approximately the same fields were photographed at 24 h. Scale bar: 100 µm (original magnification ×200). (B) Percentage of wound healing is calculated based on the healing of wounds in 24 h. *n*=3. Mean±SD. [b]$P<0.05$, [c]$P<0.01$ *vs* control L-CM group; [f]$P<0.01$ *vs* Wnt3a-CM group.

which cooperated with Wnt3a, may contribute to induce myogenesis in MSC. This will require further studies. In line with our results, one recent study reported that Wnt molecules activated the myogenic recruitment of CD45^{+} cells isolated from uninjured muscles[18]; another study suggested that the activation of Wnt signaling induced the transcription of different skeletal muscle marker genes in 2 stem cell populations isolated from adult murine bone marrow[36]. All these studies demonstrate that Wnt signaling is capable of inducing myogenesis in adult stem cells.

Recent studies have demonstrated that Wnt signaling controls the balance between myogenic and adipogenic potential in many types of adult stem cells, including myoblasts, pre-adipocytes, and C3H10T1/2 mesenchymal stem cells *in vitro* and *in vivo*[28,37,38]. Myoblasts isolated from Wnt10b–/– mice show increased adipogenic potential, likely contributing to excessive lipid accumulation in actively regenerating myofibers *in vivo*. The inhibition of the Wnt signaling pathway by the overexpression of axin, dominant-negative TCF4, or Dkk1 in 3T3-L1 pre-adipocytes and myoblasts promotes these cells to differentiate into adipocytes[28,38]. On the other hand, the activation of the Wnt signaling pathway inhibits adipogenesis[28]. Moreover, the alteration in Wnt signaling in myoblasts with age impairs muscle regenerative capacity and increases muscle adiposity[37]. These studies imply that Wnt signaling plays an important role in mesodermal cell fate determination[28]. One recent study demonstrated that the activation of the Wnt signaling pathway inhibited adipogenic differentiation in human MSC[21]. In this report, we found that Wnt3a inhibited the adipogenic differentiation in rMSC, similar to the result in human MSC. In embryogenesis, both adipocytes and myocytes are derived from mesodermal precursor cells, which have the potential to differentiate into the mesodermal cell types of adipocytes, chondrocytes, osteoblasts, and myocytes. As our results demonstrated that the activation of the Wnt signaling pathway by Wnt3a induced myogenesis and inhibited adipogenesis in rMSC, we hypothesized that the activation of Wnt signaling might direct mesenchymal stem cell fate towards myogenesis while preventing commitment to the adipogenesis.

Different types of tissue engineering have been examined using MSC in recent years. MSC have been shown to regenerate injured tissues when applied from different sites of application. However, the factors involved in the control of the migration of MSC are widely unknown at present time. It is well known that the Wnt signal is involved in cell mobility during the development and metastasis of many kinds of cancer cells[39–41]. In the present study, we analyzed the effect of Wnt signaling on the migration of MSC. The results from the transwell migration and wound healing as-

says showed that Wnt3a could promote rMSC migration. The ability of Wnt3a in stimulating the migration of rMSC is reminiscent of the recent findings that Wnt3a induced the migration of myeloma plasma cells through vascular endothelia[40]. Furthermore, activating mutations in the Wnt pathway result in extensive migration and are responsible for increased metastasis in other tumor cells[42]. Combining the results of published studies and the present study, it becomes apparent that Wnt3a is capable of promoting the migration of mesenchymal stem cells.

The ability of Wnt signaling to induce myogenic differentiation and promote proliferation and migration in rMSC may allow for its therapeutic application. Our ongoing studies aim to further examine the effect of Wnt signaling on transplanted rMSC maintenance, lineage commitment, and differentiation in the mdx mouse model of DMD. These studies could provide a rational foundation for cell-based tissue repair in humans.

Acknowledgement

References

1 Friedenstein AJ, Gorskaja JF, Kulagina NN. Fibroblast precursors in normal and irradiated mouse hematopoietic organs. Exp Hematol 1976; 4: 267–74.

2 Pittenger MF, Mackay AM, Beck SC, Jaiswal RK, Douglas R, Mosca JD, *et al*. Multilineage potential of adult human mesenchymal stem cells. Science 1999; 284: 143–7.

3 Jiang Y, Jahagirdar BN, Reinhardt RL, Schwartz RE, Keene CD, Ortiz-Gonzalez XR, *et al*. Pluripotency of mesenchymal stem cells derived from adult marrow. Nature 2002; 418: 41–9.

4 Reyes M, Lund T, Lenvik T, Aguiar D, Koodie L, Verfaillie CM. Purification and *ex vivo* expansion of postnatal human marrow mesodermal progenitor cells. Blood 2001; 98: 2615–25.

5 Price FD, Kuroda K, Rudnicki MA. Stem cell based therapies to treat muscular dystrophy. Biochim Biophys Acta 2007; 1772: 272–83.

6 Dezawa M, Ishikawa H, Itokazu Y, Yoshihara T, Hoshino M, Takeda S, *et al*. Bone marrow stromal cells generate muscle cells and repair muscle degeneration. Science 2005; 309: 314–7.

7 De Bari C, Dell'Accio F, Vandenabeele F, Vermeesch JR, Raymackers JM, Luyten FP. Skeletal muscle repair by adult human mesenchymal stem cells from synovial membrane. J Cell Biol 2003; 160: 909–18.

8 Parker MH, Seale P, Rudnicki MA. Looking back to the embryo: defining transcriptional networks in adult myogenesis. Nat Rev Genet 2003; 4: 497–507.

9 Moon RT, Kohn AD, De Ferrari GV, Kaykas A. WNT and beta-catenin signalling: diseases and therapies. Nat Rev Genet 2004; 5: 691–701.

10 Yu JM, Kim JH, Song GS, Jung JS. Increase in proliferation and

differentiation of neural progenitor cells isolated from postnatal and adult mice brain by Wnt-3a and Wnt-5a. Mol Cell Biochem 2006; 288: 17–28.

11 Gordon MD, Nusse R. Wnt signaling: multiple pathways, multiple receptors, and multiple transcription factors. J Biol Chem 2006; 281: 22 429–33.

12 Aberle H, Bauer A, Stappert J, Kispert A, Kemler R. Beta-catenin is a target for the ubiquitin-proteasome pathway. EMBO J 1997; 16: 3797–804.

13 Li L, Yuan H, Xie W, Mao J, Caruso AM, McMahon A, *et al*. Dishevelled proteins lead to two signaling pathways. Regulation of LEF-1 and c-Jun N-terminal kinase in mammalian cells. J Biol Chem 1999; 274: 129–34.

14 Munsterberg AE, Kitajewski J, Bumcrot DA, McMahon AP, Lassar AB. Combinatorial signaling by Sonic hedgehog and Wnt family members induces myogenic bHLH gene expression in the somite. Genes Dev 1995; 9: 2911–22.

15 Tajbakhsh S, Borello U, Vivarelli E, Kelly R, Papkoff J, Duprez D, *et al*. Differential activation of Myf5 and MyoD by different Wnts in explants of mouse paraxial mesoderm and the later activation of myogenesis in the absence of Myf5. Development 1998; 125: 4155–62.

16 Borello U, Coletta M, Tajbakhsh S, Leyns L, De Robertis EM, Buckingham M, *et al*. Transplacental delivery of the Wnt antagonist Frzb1 inhibits development of caudal paraxial mesoderm and skeletal myogenesis in mouse embryos. Development 1999; 126: 4247–55.

17 Ikeya M, Takada S. Wnt signaling from the dorsal neural tube is required for the formation of the medial dermomyotome. Development 1998; 125: 4969–76.

18 Polesskaya A, Seale P, Rudnicki MA. Wnt signaling induces the myogenic specification of resident CD45$^+$ adult stem cells during muscle regeneration. Cell 2003; 113: 841–52.

19 Neth P, Ciccarella M, Egea V, Hoelters J, Jochum M, Ries C. Wnt signaling regulates the invasion capacity of human mesenchymal stem cells. Stem Cells 2006; 24: 1892–903.

20 Jian H, Shen X, Liu I, Semenov M, He X, Wang XF. Smad3-dependent nuclear translocation of beta-catenin is required for TGF-beta1-induced proliferation of bone marrow-derived adult human mesenchymal stem cells. Genes Dev 2006; 20: 666–74.

21 De Boer J, Wang HJ, Van Blitterswijk C. Effects of Wnt signaling on proliferation and differentiation of human mesenchymal stem cells. Tissue Eng 2004; 10: 393–401.

22 Wakitani S, Saito T, Caplan AI. Myogenic cells derived from rat bone marrow mesenchymal stem cells exposed to 5-azacytidine. Muscle Nerve 1995; 18: 1417–26.

23 Shibamoto S, Higano K, Takada R, Ito F, Takeichi M, Takada S. Cytoskeletal reorganization by soluble Wnt-3a protein signalling. Genes Cells 1998; 3: 659–70.

24 Hyatt JP, Roy RR, Baldwin KM, Edgerton VR. Nerve activity-independent regulation of skeletal muscle atrophy: role of MyoD and myogenin in satellite cells and myonuclei. Am J Physiol Cell Physiol 2003; 285: C1161–73.

25 Armand AS, Pariset C, Laziz I, Launay T, Fiore F, Della Gaspera B, *et al*. FGF6 regulates muscle differentiation through a calcineurin-dependent pathway in regenerating soleus of adult mice. J Cell Physiol 2005; 204: 297–308.

26 Reinecke H, Poppa V, Murry CE. Skeletal muscle stem cells do not transdifferentiate into cardiomyocytes after cardiac grafting. J Mol Cell Cardiol 2002; 34: 241–9.

27 Hamdi HK, Castellon R. ACE inhibition actively promotes cell survival by altering gene expression. Biochem Biophys Res Commun 2003; 310: 1227–35.

28 Ross SE, Hemati N, Longo KA, Bennett CN, Lucas PC, Erickson RL, *et al*. Inhibition of adipogenesis by Wnt signaling. Science 2000; 289: 950–3.

29 de Boer J, Siddappa R, Gaspar C, van Apeldoorn A, Fodde R, van Blitterswijk C. Wnt signaling inhibits osteogenic differentiation of human mesenchymal stem cells. Bone 2004; 34: 818–26.

30 Pinto D, Clevers H. Wnt control of stem cells and differentiation in the intestinal epithelium. Exp Cell Res 2005; 306: 357–63.

31 Nguyen H, Rendl M, Fuchs E. Tcf3 governs stem cell features and represses cell fate determination in skin. Cell 2006; 127: 171–83.

32 Lie DC, Colamarino SA, Song HJ, Desire L, Mira H, Consiglio A, *et al*. Wnt signalling regulates adult hippocampal neurogenesis. Nature 2005; 437: 1370–5.

33 Reya T, Duncan AW, Ailles L, Domen J, Scherer DC, Willert K, *et al*. A role for Wnt signalling in self-renewal of haematopoietic stem cells. Nature 2003; 423: 409.

34 Wagner J, Schmidt C, Nikowits W Jr, Christ B. Compartmentalization of the somite and myogenesis in chick embryos are influenced by wnt expression. Dev Biol 2000; 228: 86–94.

35 Petropoulos H, Skerjanc IS. Beta-catenin is essential and sufficient for skeletal myogenesis in P19 cells. J Biol Chem 2002; 277: 15393–9.

36 Belema Bedada F, Technau A, Ebelt H, Schulze M, Braun T. Activation of myogenic differentiation pathways in adult bone marrow-derived stem cells. Mol Cell Biol 2005; 25: 9509–19.

37 Vertino AM, Taylor-Jones JM, Longo KA, Bearden ED, Lane TF, McGehee RE Jr, *et al*. Wnt10b deficiency promotes coexpression of myogenic and adipogenic programs in myoblasts. Mol Biol Cell 2005; 16: 2039–48.

38 Christodoulides C, Laudes M, Cawthorn WP, Schinner S, Soos M, O'Rahilly S, *et al*. The Wnt antagonist Dickkopf-1 and its receptors are coordinately regulated during early human adipogenesis. J Cell Sci 2006; 119: 2613–20.

39 Pinto D, Clevers H. Wnt, stem cells and cancer in the intestine. Biol Cell 2005; 97: 185–96.

40 Qiang YW, Walsh K, Yao L, Kedei N, Blumberg PM, Rubin JS, *et al*. Wnts induce migration and invasion of myeloma plasma cells. Blood 2005; 106: 1786–93.

41 Brabletz T, Hlubek F, Spaderna S, Schmalhofer O, Hiendlmeyer E, Jung A, *et al*. Invasion and metastasis in colorectal cancer: epithelial-mesenchymal transition, mesenchymal-epithelial transition, stem cells and beta-catenin. Cells Tissues Organs 2005; 179: 56–65.

42 Reya T, Clevers H. Wnt signalling in stem cells and cancer. Nature 2005; 434: 843–50.